

2. Palmer Station (06/01/22 – 05/31/23)

This sections describes quality control of solar data recorded at Palmer Station between 06/01/22 and 05/31/23. The period resulted in a total of 12,893 solar scans, which were assigned to Volume 32.

Solar data of the reporting period were affected by multiple issues:

- Instability in the responsivity of the SUV-100 spectroradiometer
 The diffuser of the SUV-100 spectroradiometer was either punctured close to the start of the reporting period or already during the previous period (2021/22), most likely by a Snowy Sheathbill pecking on it. As a result, water was able to get into the instrument’s collector, which caused large changes in the responsivity of the system until the diffuser was replaced on 4/6/23. Changes in responsivity were assessed by comparing data from the SUV-100 with measurements of the collocated GUV-511 radiometer and radiative transfer modeling. These comparisons show that changes in responsivity exceeded $\pm 20\%$ on some days, which could not be corrected and led to data loss (Section 2.4). However, for the majority of the affected period, the responsivity varied within reasonable limits and SUV-100 calibrations could be adjusted with the help of GUV-511 data. This correction assumed that the GUV-511 instrument was stable between calibration scans of the SUV. Specifically, subperiods for which the ratio of GUV-511 and SUV-100 measurements was approximately constant were selected. For each of these period, the medians of the ratios of uncalibrated GUV-511 and SUV-100 data at the GUV’s wavelengths were calculated and these values were linearly interpolated to the wavelengths measured by the SUV. For some periods (Table 1), the SUV-100 could be calibrated in the regular fashion using one or more “absolute” scans of the external calibration lamp. For periods where this was not possible, SUV-100 data were scaled accordingly using the interpolated ratios of GUV-511 and SUV-100 measurements.

Data analysis further revealed that the cosine error of the instrument’s diffuser changed considerably throughout the reporting period, likely as a consequence of the punctured diffuser. It was therefore not possible to establish new correction functions for the instrument’s cosine error and its dependence on the azimuth angle. Version 2 data were scaled up by a factor of 1/0.95, which is the correction factor that is applied when the sky is overcast and diffuse. Because UV-B radiation is mostly diffuse, regardless of whether the Sun is visible or not, the factor is a good approximation of the actual correction factor for wavelengths in the UV-B range and the factor is still acceptable for the UV-A range. However, the correction with a wavelength-independent factor becomes too uncertain for wavelengths larger than 400 nm. **Data affected by instabilities with wavelengths beyond 400 nm were therefore removed from the Version 2 dataset.** (They remain part of the Version 0 dataset, which is not corrected for the cosine error).

The uncertainty of the cosine error correction functions for wavelengths larger than ~400 nm plus the instability of the responsivity also affected the determination of cloud optical depth (which is based on measurements at 450 nm) and surface albedo. **Data of cloud optical depth and surface albedo are therefore not available until 4/6/23.**

- Change in the scan frequency after Windows update
 After a “major” upgrade of the Windows 10 Operating System on 1/18/21, communication between the system’s control computer and peripheral electronics slowed down considerably. As a consequence, spectral scans lasted longer than 15 minutes and the standard schedule of four scans per hour could no longer be maintained. Instead, measurements were performed on top of the hour and at 20 and 40 minutes past the hour. The problem was corrected on 2/8/23 when the serial port adapter that is integral to the computer was replaced with a modern USB-to-serial adapter. From 2/10/23 onward, the system is now again performing four scans per hour.

- Failure of the 320 nm channel of the GUV-511 radiometer
 The 320 nm channel of the system's GUV-511 became defective sometime at the start of the reporting period, resulting in large non-linearity. Solar data of the GUV-511 radiometer had to be produced without using the 320 nm channel. Thus, UV data products are based on measurements of the 305, 340, and 380 nm channels only. Comparisons with data from SUV-100 spectroradiometer confirmed that the quality of minute-by-minute data in "GUV2" files (specifically files PAL_v32_2022_GUV2.zip and PAL_v32_2023_GUV2.zip) is still adequate. However, "GUV1" data that are coinciding with SUV-100 measurements (PAL_v32_2022_GUV1.zip and PAL_v32_2023_GUV1.zip) show large fluctuations during cloudy conditions. **Data products that rely on measurements of all three channels (specifically data labeled "Dose1", "Dose2", "CIE", "UVIndex", "Erythema_Anders", "RBM501", "SCUP-h", "SCUP-m", "Flint", "Boucher", "Cullen_phaerodactylum", Cullen_prorocentrum", and "Neale_Antarctic") were removed from the "GUV1" files.** Data products that are based on measurements of only two channels are less impacted and were included in the data files but are also less accurate than historically. In summary, it can be concluded that "GUV2" data can be used, for example, to fill in gaps in SUV-100 data, but "GUV1" data should not be used.

The system's PSP radiometer was unit 30450F3 and has a calibration factor of $8.885 \times 10^{-6} \text{ V}/(\text{W m}^{-2})$, which was established on 11/1/17. TUVR data were erratic and were not published.

2.1. Irradiance Calibration

On-site standards

The on-site irradiance standards for the reporting period were the lamps 200W007, M700, M765, 200WN009, and 200WN010. Lamps 200WN009, and 200WN010 are "long-term" standards, which were left at Palmer Station during the March 2014 site visit. It is the intent to run lamp 200WN009 once per year to compare with the other on-site standards. 200WN010 is typically run every other year during site visits when all on-site lamps and the traveling standard are compared with each other. Both long-term standards were used twice during the reporting period.

Long-term standards

The long-term standards 200WN009 and 200WN010 were calibrated on 12/20/2013 against lamps 200WN001 and 200WN002; see the last Operations Report for details.

Working standards

The working standards 200W007, M700, M765 were recalibrated during the preparation of Volume 28. A comparison of the scale of spectral irradiance of all lamps on 4/11/23 suggested that the scale of lamp 200W007 had drifted by 0.5–1.0% relative to the scales of the other four lamps. This conclusion is also supported by the difference seen in the results of 4/11/23 and those of a similar comparison performed on 3/25/19. The lamp was recalibrated against the average scale of working standards M700 and M765. The scales of irradiance of all other lamps are the same as those applied to Volumes 28–31.

Adjustment of calibration scale

In early 2020, the chain of calibrations applied between 1996 and 2019 to solar data of the NSF and NOAA monitoring networks was re-evaluated (Bernhard and Stierle, 2020). This analysis suggested that the scale of spectral irradiance of NIST standard F-616, which has been used as the primary standard since 2013, is low compared to the scale of primary standards used before 2013. This bias is –2% at 300 nm, –1% at 375 nm, and less than $\pm 0.5\%$ between 420 and 600 nm. **Version 2 solar data of Volume 32 were scaled upward accordingly; however, Version 0 remain traceable to the original scale of the primary standard F-616.**

Comparison of calibration lamps

Figure 1 shows a comparison of the scales of spectral irradiance of all lamps used during the reporting period relative to the average scale of all lamps, which was performed on 4/11/23. (The new scale of lamp 200W007 was used). All scales agree to within $\pm 1\%$. Of note, the scales of the two long-term standards is

different by 0.9% on average for the wavelength range 290–600 nm. A similar bias between the two lamps was also observed in the past. This indicates that the scales of the two lamps has not drifted; instead, there is a small difference, which has always existed and which is within the uncertainty of the lamp’s calibrations.

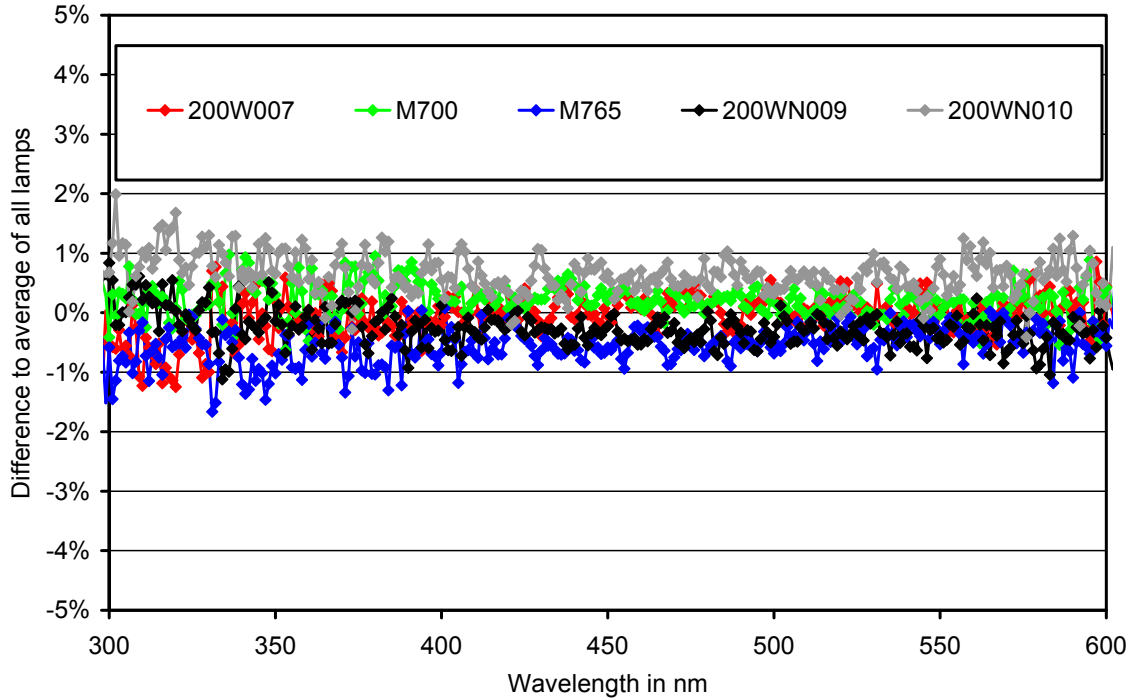


Figure 1. Comparison of the calibration of on-site and long-term standards on 4/11/23.

To further validate the irradiance scale of solar measurements of the SUV-100 spectroradiometer, the GU-511 radiometer was vicariously calibrated against SUV-100 measurements after removing all SUV-100 data that are affected by the instrument’s instability described above. Calibration factors calculated with this method were compared with similar factors established during previous years. The analysis showed that calibration factors for the GU-511’s 305, 340, and 380 channels were larger by 0.3%, 0.4%, and –1.2%, respectively, compared to similar factors established for data of the 2021/22 period. This result confirms the good consistency of SUV-100 calibrations of the 2021/22 and 2022/23 periods despite the instability affecting the latter period.

2.2. Instrument Stability

The radiometric stability of the SUV-100 spectroradiometer was monitored with calibrations utilizing the on-site irradiance standards, with daily “response” scans of the internal lamp, by comparison with measurements of the collocated GU-511 multifilter radiometer, and by comparisons with results of a radiative transfer model (part of “Version 2” data, see Bernhard et al. (2004)).

Figure 2 shows results from measurements of the internal lamp. Specifically, readings of the instrument’s TSI sensor (a filtered photo diode with sensitivity mostly in the UV-A) are compared with measurements of the SUV-100’s PMT at 300 and 400 nm, derived from response scans performed between 6/1/22 and 5/31/23. TSI measurements decreased by about 2% during this period, indicating that the internal lamp became dimmer by this amount. (Fluctuation at the 0.5% level in the TSI measurements are the result of the resolution of the digitally-controlled 12-bit power supply that powers the lamp.) PMT currents at 300

and 400 nm decreased by about 3%. However, the fluctuations of PMT currents are substantially larger than the variation in the TSI signal, suggesting variations in either the monochromator’s throughput or the PMT’s sensitivity. By “pairing” solar scans of a particular day with the response scan of that day, most of these fluctuations are removed. **Of note, the variabilities indicated in Figure 2 quantify instabilities of internal optics only. They do not track changes in responsivity resulting from the punctured diffuser.**

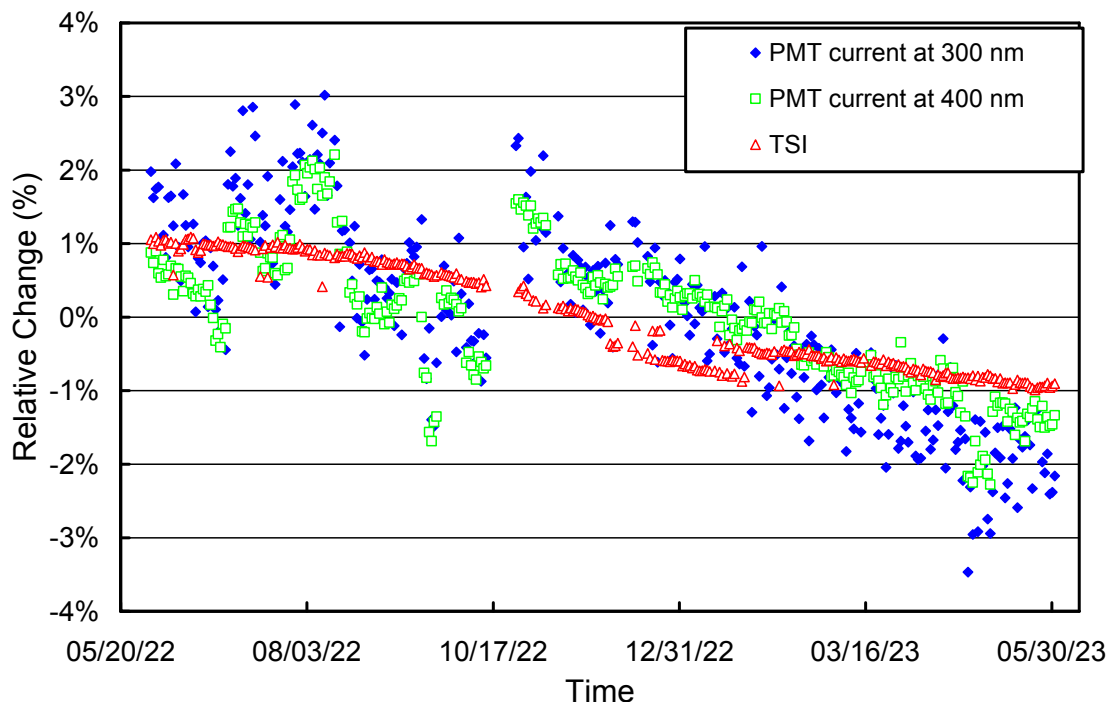


Figure 2. Time-series of PMT current at 300 and 400 nm, and TSI signal. All data were extracted from measurements of the internal irradiance standard and are normalized to their average.

The reporting period was divided into an unprecedented number of 34 calibration periods due to the large variations in responsivity resulting from the punctured diffuser. An overview of these periods is provided in Table 1. Figure 3 shows ratios of the calibration functions applied during Periods P1 through P16 relative to the function of Period P1.

Table 1. Calibration periods for Palmer Volumes 32.

Period name	Period range	Number of absolute scans	Remarks
P1	06/01/22 – 06/30/22	2	Standard calibration
P2	07/01/22 – 07/08/22	3	Standard calibration
P3	07/09/22 – 08/20/22	3	Standard calibration
P4	08/21/22 – 09/24/22	2	Standard calibration
P4A	09/26/22 – 09/29/22	0	Scaled; based on P4
P4B	09/30/22 – 10/04/22	0	Scaled; based on P4
P5	10/06/22 – 10/10/22	1	Standard calibration
P5A	10/11/22 – 10/12/22	0	Scaled; based on P5
P5B	10/13/22 – 10/14/22	0	Scaled; based on P5
P6A	10/26/22 – 10/30/22	0	Scaled; based on P6
P6B	10/31/22 – 11/03/22	0	Scaled; based on P6
P6	11/04/22 – 11/07/22	1	Standard calibration
P7	11/12/22 – 11/21/22	1	Standard calibration
P8A	11/22/22 – 11/22/22	0	Scaled; based on P8

P8B	11/23/22 – 11/25/22	0	Scaled; based on P8
P8C	11/26/22 – 11/29/22	0	Scaled; based on P8
P8	11/30/22 – 12/06/22	1	Standard calibration
P8D	12/12/22 – 12/14/22	0	Scaled; based on P8
P8E	12/15/22 – 12/16/22	0	Scaled; based on P8
P9A	12/17/22 – 12/17/22	0	Scaled; based on P9
P9	12/18/22 – 12/31/22	1	Standard calibration
P9B	01/01/23 – 01/06/23	0	Scaled; based on P9
P9C	01/07/23 – 01/10/23	0	Scaled; based on P9
P10	01/11/23 – 01/25/23	1	Standard calibration
P11	01/26/23 – 01/31/23	0	Scaled; based on P10
P11A	02/01/23 – 02/05/23	0	Scaled; based on P10
P11B	02/06/23 – 02/06/23	0	Scaled; based on P10
P11C	02/07/23 – 02/07/23	0	Scaled; based on P10
P11D	02/08/23 – 02/08/23	0	Scaled; based on P10
P12	02/09/23 – 3/10/23	0	Scaled; based on P10
P13	03/11/23 – 03/16/23	1	Standard calibration
P14	03/17/23 – 04/04/23	3	Standard calibration
P15	04/05/23 – 04/21/23	5	Standard calibration
P16	04/22/23 – 05/31/23	4	Standard calibration

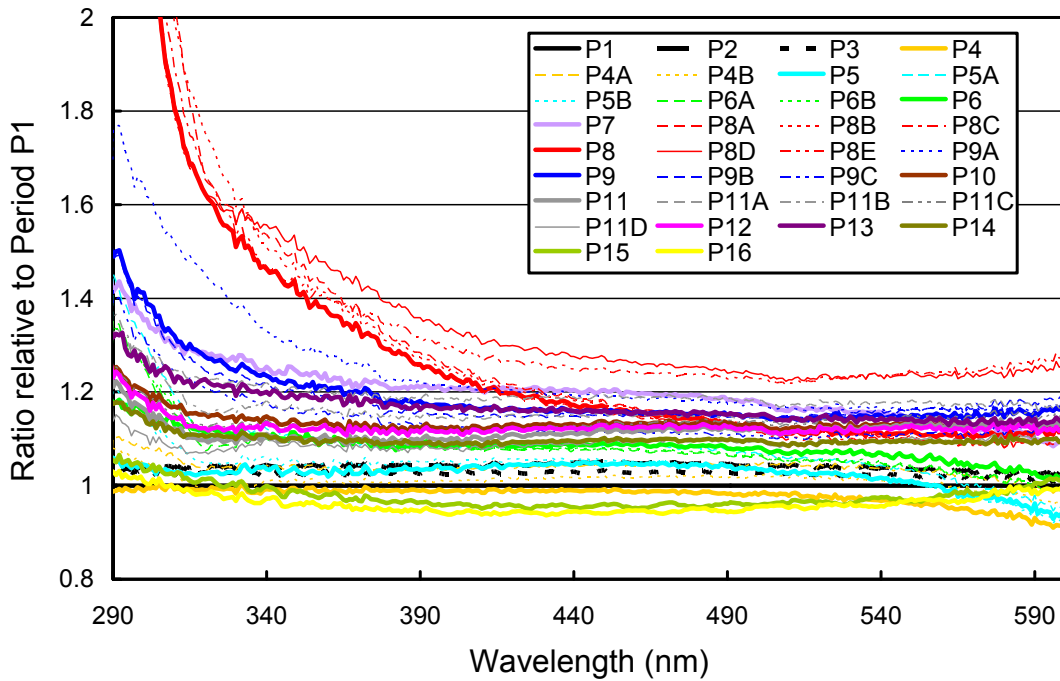


Figure 3. Ratios of spectral irradiance assigned to the internal reference lamp for periods P1 – P16, relative to Period P1. Functions that were established using standard calibration methods are printed in bold. Functions that were derived by scaling with GUV-511 data are indicated by thin lines.

Figure 4 shows the ratio of GUV-511 data (340 nm channel) and final SUV-100 measurements, which were weighted with the spectral response function of this channel. The ratio is normalized and should ideally be one. With the exception of a few outliers, GUV-511 and SUV-100 measurements agree to

within $\pm 10\%$. The standard deviation is 0.028. For comparison, the standard deviation of similar data of the previous period (Vol31; 2021/22) was 0.031, indicating that the uncertainty of SUV-100 data of the current period that were included in the published dataset is similar to that of the previous period.

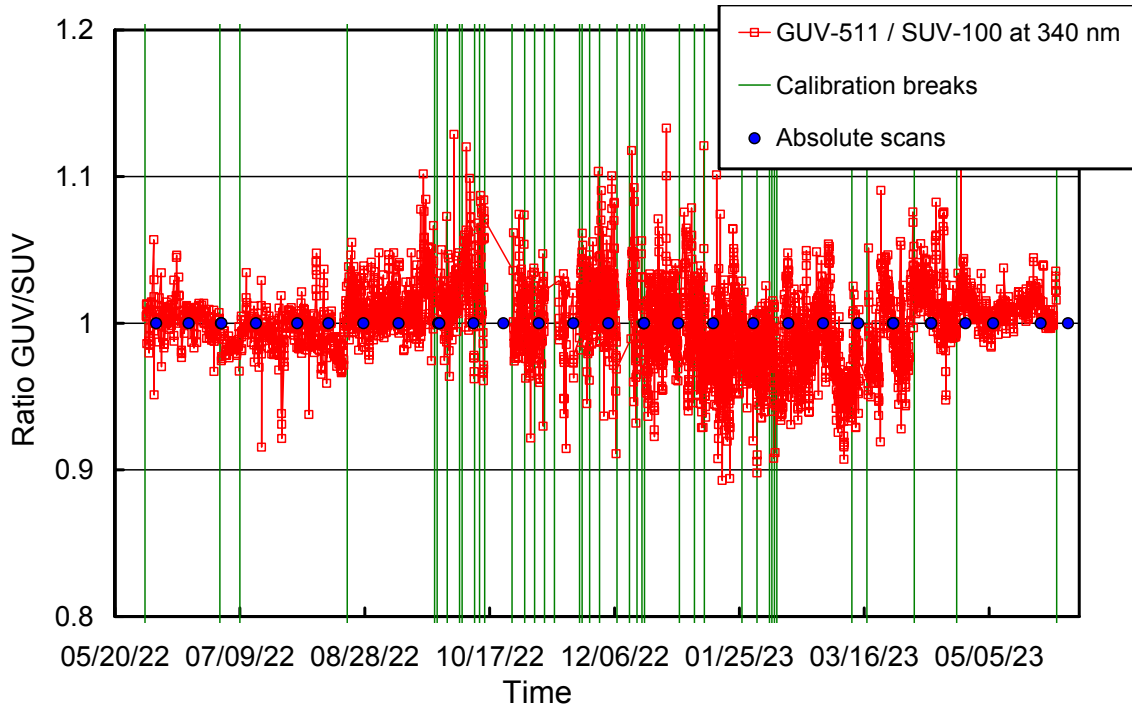


Figure 4. Ratio of GUV-511 measurements at 340 nm with SUV-100 measurements. The latter were weighted with the spectral response function of the GUV-511’s 340 nm channel.

2.3. Wavelength Calibration

Wavelength stability of the system was monitored with the internal mercury lamp. Information from the daily wavelength scans was used to homogenize the data set by correcting day-to-day fluctuations in the wavelength offset. The wavelength-dependent bias of this homogenized dataset and the correct wavelength scale was determined with the Version 2 Fraunhofer-line correlation method (Bernhard et al., 2004). Figure 5 shows the correction function calculated with this algorithm. Figure 6 indicates the wavelength accuracy of Version 0 data for five wavelengths in the UV and visible range, obtained by running the Fraunhofer-line correlation method for a second time. Shifts are typically smaller than ± 0.1 nm. (The standard deviations for wavelengths between 305 and 400 nm are 0.033 nm on average). There are several steps in this time series. Some are caused by the system’s monochromator losing its wavelength position due to the communication problem between the computer and Spectralink module. The wavelength accuracy was further improved as part of the production of Version 2 data. Figure 7 shows the wavelength accuracy of Version 2 data. There are no step-changes and the standard deviations for wavelengths between 305 and 400 nm decreased to 0.025 nm.

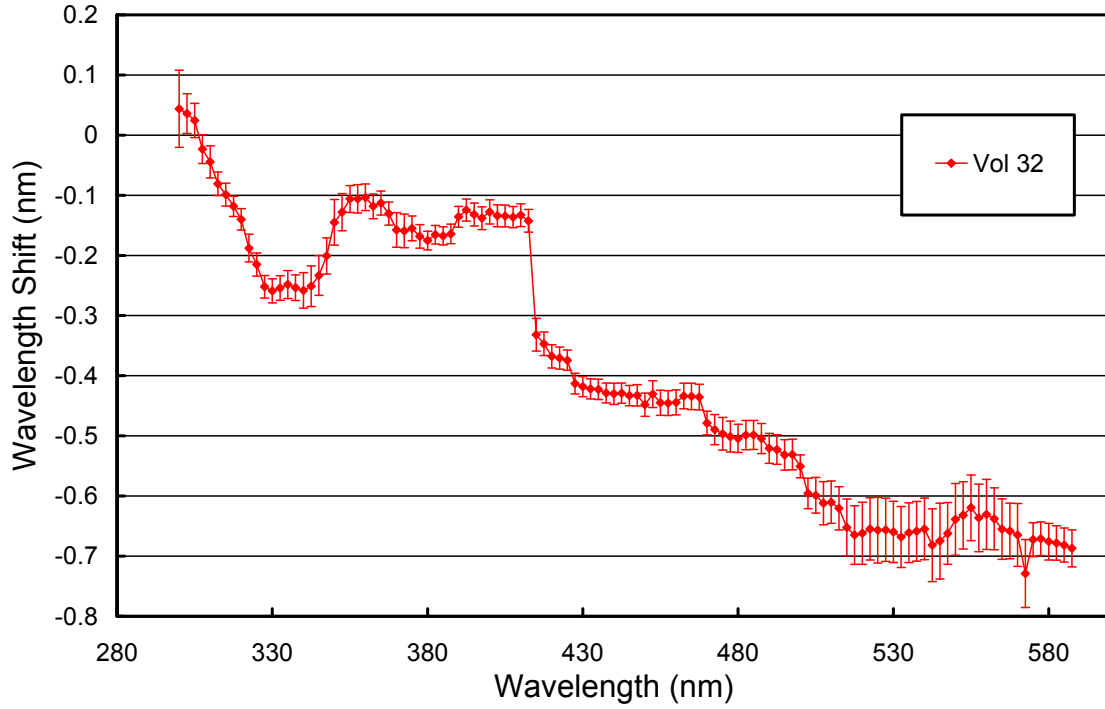


Figure 5. Monochromator mapping function. Error bars indicate 1- σ variation.

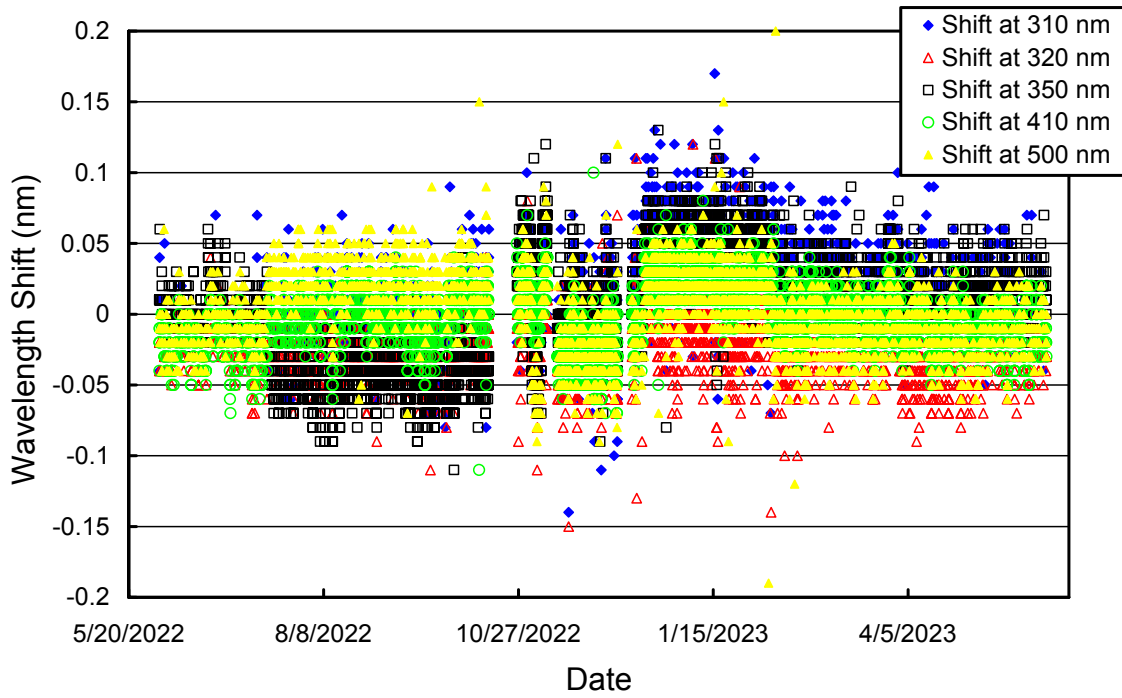


Figure 6. Wavelength accuracy check of *Version 0* data at five wavelengths by means of Fraunhofer-line correlation. Measurements were evaluated in hourly increments.

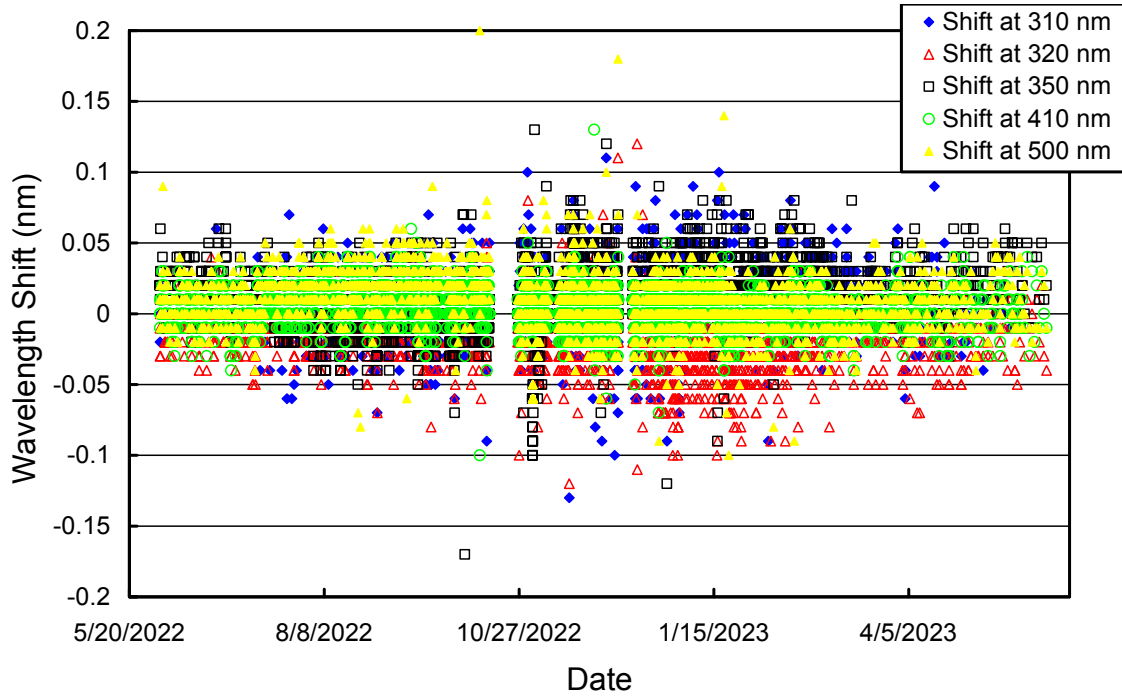


Figure 7. Same as Figure 6 but for *Version 2* data.

2.4. Missing data

Table 2 provides a list of missing days in the published dataset. Almost all data gaps are caused by instabilities in the instrument’s responsivity that could not be corrected.

Table 2. Days with no data.

Date	Date
09/11/22	11/17/22 – 11/18/22
09/25/22 – 09/26/22	11/20/22 – 11/21/22
10/05/22	12/07/22 – 12/11/22
10/15/22 – 10/25/22	12/15/22
11/04/22	12/17/22
11/08/22 – 11/12/22	02/09/23
11/14/22	03/14/23 – 03/16/23

References

Bernhard, G., C. R. Booth, and J. C. Eshamjian. (2004). Version 2 data of the National Science Foundation’s Ultraviolet Radiation Monitoring Network: South Pole, *J. Geophys. Res.*, 109, D21207, doi:10.1029/2004JD004937.

Bernhard G. and S. Stierle (2020). Trends of UV Radiation in Antarctica, *Atmosphere*, 11(8), 795, doi: https://doi.org/10.3390/atmos11080795.